Comparison of variations in air mass attraction derived from radiosonde data and a meteorological weather model

D. Simon[1], Th. Klügel[2], and C. Kroner[3]

[1] Frankensteinstr.4, D-36469 Tiefenort, Germany, formerly: Federal Agency for Cartography and Geodesy, Frankfurt a.M.

[2] Federal Agency for Cartography and Geodesy, Fundamental Station Wettzell, Sackenrieder Str. 25, D-93444 Bad Kötzting, Germany

[3] Institute of Geosciences, Burgweg 11, 07749 Jena, Germany

Abstract

For several years now endeavours are undertaken to improve the reduction of barometric pressure effects in continuous gravity observations. It is expected that a further improvement can be achieved by a more sophisticated consideration of the attraction effect of air mass fluctuations in a local to regional area around a gravimeter site. Two different approaches are compared for a number of stations: the computation of the attraction effect from radiosonde data and from a local high-resolution meteorological weather model. Differences in the two modelling approaches are discussed. First tentative explanations for deviations in the resulting attraction effects are given.

1. Objectives of the model comparison

For the computation of the gravimetric effect of air mass shifts often data of global meteorological models have been used besides classical regression reductions (e.g. MERRIAM, 1992; SUN, 1995; SUN ET AL., 1995; KRONER & JENTZSCH, 1999; NEUMEYER ET AL., 2004; BOY ET AL., 2002). A disadvantage of these model data is their small spatial resolution. Typically the grid distance is 0.5° which esp. affects the accuracy of the computed attraction component $A_p(t)$. $A_p(t)$ denotes the surface pressure dependent component of the total attraction effect $A(t)$ and is given as $A_p(t)=A(t)-A_c(t)$ (Simon, 2002, 2003). It is caused by horizontal air mass movements, which cover a broad spatial and temporal spectral range. $A_c(t)$ denotes the component being independent of surface pressure.

According to KRONER (1997) it might be necessary to install several air pressure and temperature sensors in a local zone of about 50 km radius around a gravimeter site in order to determine the component $A_p(t)$ with an improved accuracy. An alternative was suggested in SIMON (2003) in order to improve the horizontal resolution: to use the local model LM of the German Meteorological Service (DWD) for the computation of the attraction component. The horizontal resolution of the model is about 14 km. 35 vertical layers with 36 layer boundaries are considered. The time resolution is 4 values per day. Using LM data KLÜGEL (2003) had already calculated the attraction effect for the gravimeter station Wettzell for a period of 16 days. With the support of the Federal Agency for Cartography and Geodesy (BKG) and in the frame of a joint project these computations were extended by KLÜGEL for the complete year 2003. The contributions $A(t)$, $A_p(t)$, and $A_c(t)$ were computed for three locations of superconducting gravimeters (Wettzell, Bad Homburg, and Moxa) and two radiosonde stations (Meiningen and Munich).

In the next step the obtained model curves of air mass attraction should be compared with model curves derived from global meteorological models, radiosonde data, and the additional deployment of data from a local pressure network. On the basis of such a comparison a better estimate of the uncertainties in the modelling and an improved modelling should be achievable.

From a first comparison emerged that for all five stations for which a reduction based on radiosonde data was calculated the amplitudes of the $A_c(t)$-curve were 2.2 times larger than the amplitudes obtained using LM data. In the computations using radiosonde data a cylin-

drical air column with a radius of 113 km and a height of 31 km was considered. The model area for the LM data covered the same area, but the height of the air column was 23.6 km. For the elimination of the surface pressure proportional component $A_p(t)$ in the total attraction effect $A(t)$ an air pressure coefficient of 0.35 µGal/hPa had to be usedinstead of 0.4 µGal/hPa for the radiosonde data. Multiplying the $A_c(t)$-curve derived from LM data by a factor of 2.2 yielded a good correspondence to the curves obtained with radiosonde data. The good agreement is found for both, annual variations and shorter-periodic contributions (SIMON, 2006).

2. Model differences as the origin of the factor 2.2

The systematic difference of the factor 2.2 between the model curves could be caused by different approaches or assumptions in the modelling. The main difference between the two model approaches is the following:

In the case of the model based on radiosonde data (SIMON, 2003) the variation of the air mass attraction due to warming / cooling of the air masses is computed for a circular-cylindrical air mass body with the vertical axis running through the location of the radiosonde station. The air pressure changes only vertically as observed with the radiosonde, and not laterally. This assumption only marginally changes the effect of the seasonal warming / cooling of the air layers on the computed attraction curves $A_c(t)$ of the air cylinder. The seasonal warming / cooling occurs in a very similar way for locations with a maximum distance of 226 km. The changes in the model cylinder will not differ much from those in the real air volume above the radiosonde station. The same assumption reduces the influence of horizontal air mass shifts on the total result.

The component $A_p(t)$ can even be totally eliminated in $A(t)$ because of the lateral constance of air pressure in the model cylinder. For separation of the component $A_p(t)$ the surface pressure curve is simply multiplied by an empirically determined air pressure coefficient r (here 0.4 µGal/hPa) and subtracted from $A(t)$. For the attraction component $A_c(t)_{radiosonde}$ follows:

$$A_c(t)_{radiosonde} = A(t)_{radiosonde} - r * p(t)) \tag{1}$$

$A_c(t)_{radiosonde}$: surface pressure independent component of $A(t)$ in µGal
$p(t)$: surface pressure in hPa
$A(t)_{radiosonde}$: total attraction effec in µGal
r: regression coefficient in µGal/hPa.

In the model used by KLÜGEL (2003) the total volume around the considered station is divided into 225 rectangular piles each having a base of $14 * 14$ km², thus covering the same area than the radiosonde model. Each pile consists of 35 layers reaching a total height of 23.6 km. The surface pressure is different at each grid point . The differences become larger with increasing distance.

The total attraction $A(t)$ at the observation point (radiosonde station) is computed in this model by summing up all n contributions $A_n(t)$

$$A(t)_{LM} = \Sigma_n A_n(t). \tag{2}$$

The contributions $A_n(t)$ of the 225 piles to the total effect have similar $A_{cn}(t)$-components, but their $A_{pn}(t)$-contributions differ due to to the lateral variations of the surface pressure. Thus a difference emerges between the curve $A(t)_{LM}$ computed according to (2) and $A(t)_{radiosonde}$

$$A(t)_{LM} <> A(t)_{radiosonde.} \tag{3}$$

In order to determine the total attraction effect A(t) from $A_c(t)_{LM}$, which could better be compared to $Ac(t)_{radiosonde}$, it would have been necessary to compute the $A_{cn}(t)$ of the seasonal warming / cooling of the air masses from the partial attractions $A_n(t)$ and pressure functions $p_n(t)$ at each of the 225 grid locations

$$A_{cn}(t) = A_n(t) - A_{pn}(t) = A_n(t) - r_n{}^* p_n(t). \tag{4}$$

From the sum of the attraction components

$$A_c(t)_{LM} = \Sigma_n A_{nc}(t) \tag{5}$$

the required attraction component $A_c(t)$ would follow. The attraction component $A_c(t)_{LM}$ is actually determined from the total attraction $A(t)_{LM}$ using the pressure curve p(t) from the observation point (radiosonde station)

$$A_c(t)_{LM} = A(t)_{LM} - r * p(t). \tag{6}$$

The annual wave thus obtained is too small. The quantitative consequences of the model difference on the attraction component $A_c(t)$ cannot be estimated yet. For verification extensive software modifications are necessary which are not realised up to now. The effects of other model differences on the computed air mass attraction could already be quantified. They partly explain the observed discrepancy between the two model approaches. The results of these studies are summarized in the following. The influence of the area extension and the neglection of the curvature of the earth in the model by Simon are not discussed here. A comprehensive discussion is given in the publications by SUN (1995) and SIMON (2003).

3. Additional sources for deviations

One additional verification is to check whether the same mean density values for the 35 air layers can be obtained using the same mean virtual temperatures from the meteorological model LM. The second question is whether these density values together with the model by Simon would yield different $A(t)_{LM}$ curves which are closer to the curves derived from radiosonde data.

3.1. Comparison of air density and latitude-dependent variation of earth acceleration

These test computations were carried out using LM data from one radiosonde station (Meiningen), for which already the air mass attraction A(t) and its components $A_c(t)$ and $A_p(t)$ had been calculated. At these stations also observed surface pressure data are available for comparison.

From the meteorological model the time series (6 h sampling rate) for the mean virtual temperature within all 35 air layers, the height of the layer boundaries and the pressure at the model surface can be obtained. The height of this surface typically deviates from the real earth's surface by some meters . At first the surface pressure curve for the real station height and the pressure variations for the 35 air layers were computed. In a second step the air density variations were calculated from these data using virtual temperatures.

For the computation of the air pressure at the boundary layers the actual gravity acceleration is required, which is a function of latitude and height. In the LM data based model the latitude-dependence of g was neglected and a constant average value for g has been used.

The consideration of this dependence of g leads to an increase in the peak-to-peak amplitude of the attraction effect A(t) and its two components $A_p(t)$ and $A_c(t)$ by 1-2% at maximum.

This increase results from air density differences of up to 11 g/m³, which esp. occur in layers with heights between 4000 and 10000 m. They correlate with mean reductions in the pressure magnitde at the upper and lower boundary of the layer. The mean air pressure e.g. diminishes by about 7 hPa in 5000-10000 m (Fig. 1).

Subtraction of the attraction component $A_p(t)=0.38$ [µGal/hPa]*p(t) [hPa] from the improved total attraction curve A(t) leads to the attraction component $A_c(t)$ caused by the seasonal warming / cooling of the air masses

$$A_c(t) = A(t) - A_p(t) = A(t) - r*p(t). \qquad (7)$$

The resulting $A_c(t)$-curve contains an annual wave with a peak-to-peak amplitude of about 2.4 µGal (Fig. 2). It is thus by a small amount larger than the one obtained from radiosonde data (1.8 µGal).

3.2. Effect of seasonal mass shifts in different heights

The LM and radiosonde data sets can be used to show how seasonal air density variations in certain heights contribute to the total effect. To investigate this an air mass package in a height of 23.6 km was divided into three parts. Each of these three volumes contributes about 1/3 to the total attraction effect A(t). The thicknesses of the volumes are 2997, 4867, and 15274 m. The corresponding air pressure coefficients are 0.18 µGal/hPa, 0.12 µGal/hPa, and 0.08 µGal/hPa. Thus it is ascertained to retrieve the coefficient of 0.38 µGal/hPa obtained for A(t)

$$A_c(t) = A(t) - 0.38*p(t) = (A_l(t)+A_m(t)+A_u(t)) - (0.18+0.12+0.08) * p(t) \qquad (8)$$

$A_l(t)$, $A_m(t)$, $A_u(t)$: contribution of the three layer packages to the total attraction effect

From Fig. 3 it becomes clear that during the summer months the air mass attraction increases in the 15 km thick upper layer. This increase compensates only partly the associated decrease
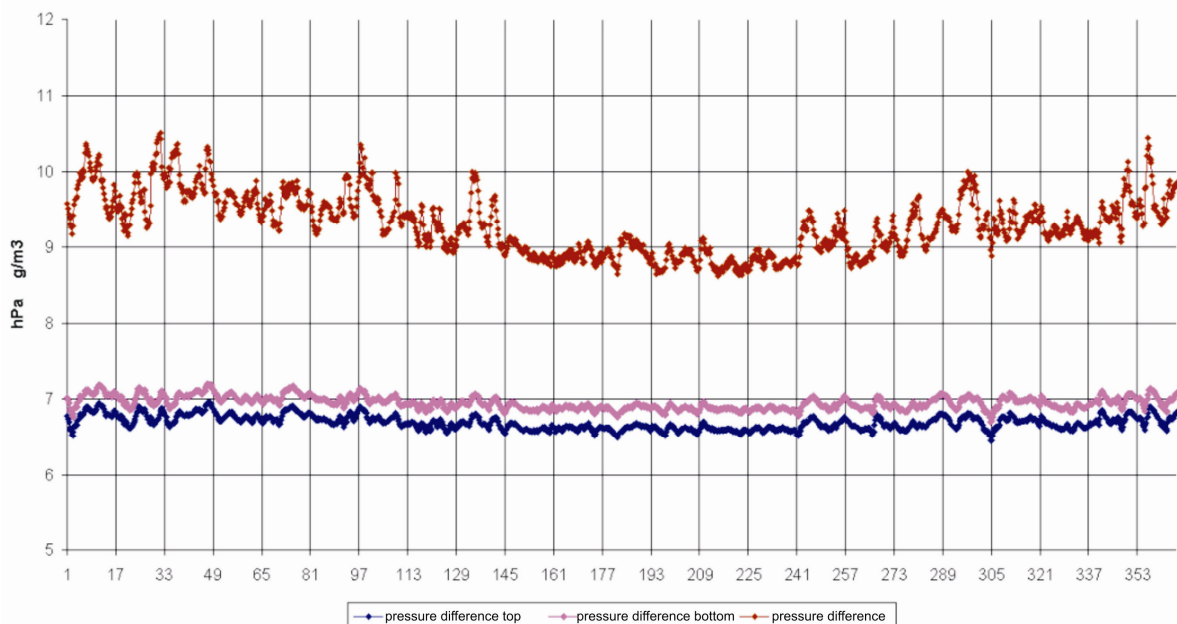

Fig. 1. Taking into account the latitude-dependence of g the mean air pressure reduces by 7 hPa and the mean air density by 13.8% in the layer 20 (5289 m- 5817 m), station Meiningen, year 2003.
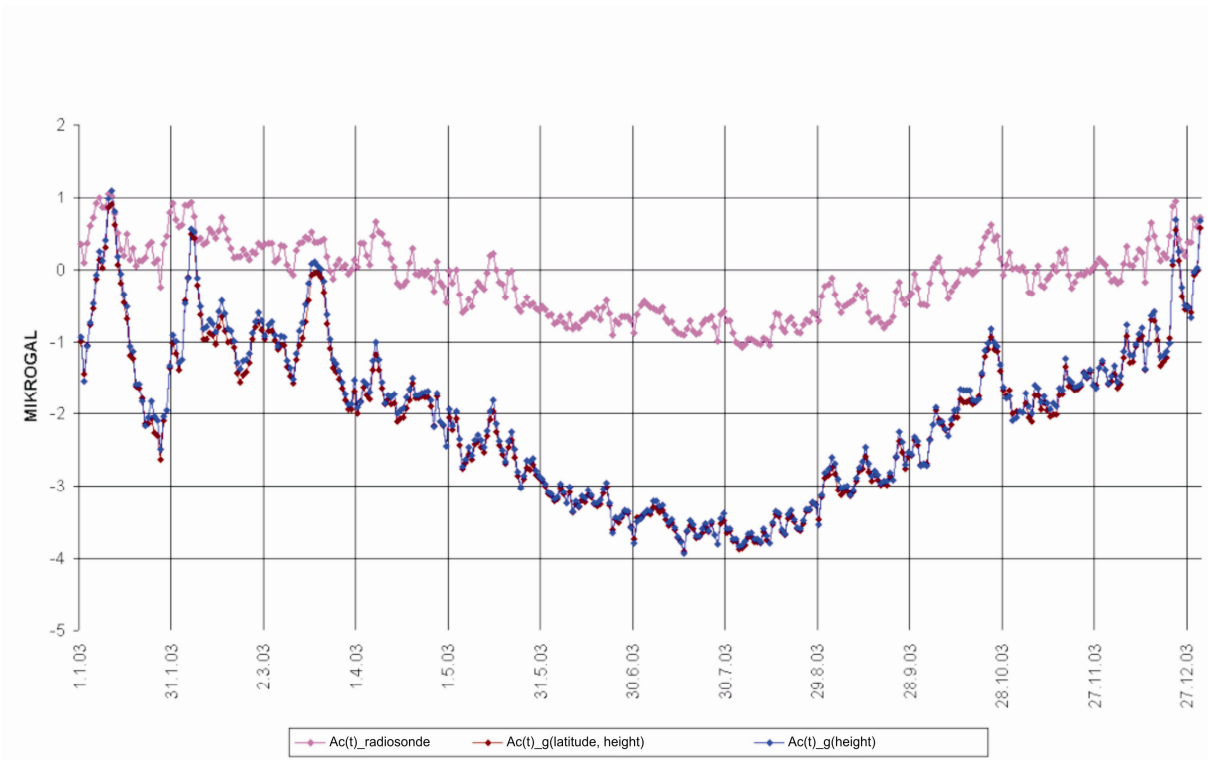
Fig. 2. Comparison of attraction component $A_c(t)$ derived from radiosonde and LM data, station Meiningen, year 2003.
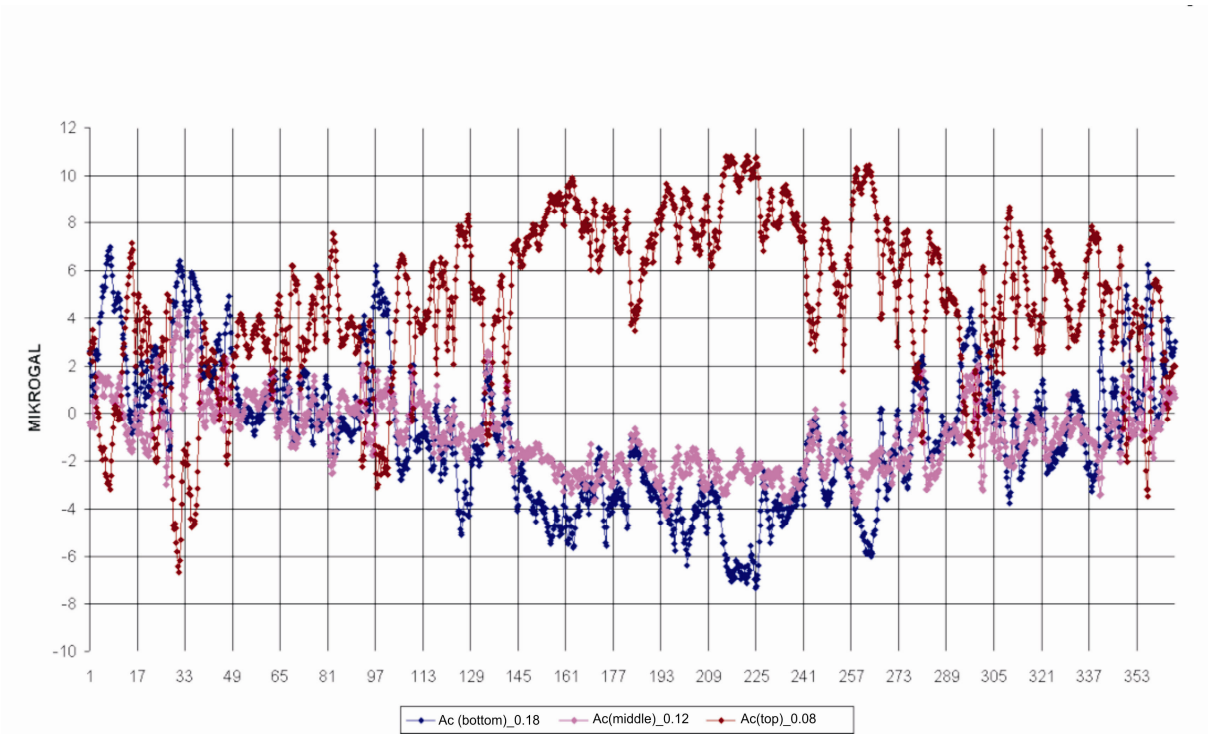

Fig. 3. Contribution of lower, middle, and upper air layer packages to the attraction component $A_c(t)$. The sum is given in Fig. 2 (lower curve); station Meiningen, year 2003.

in the lower and middle layers. This season-related decrease of the total attraction effect might be further reduced when considering an additional air mass package above 23.6 km in the modelling. In the radiosonde model the air mass cylinder is 7.4 km higher. NEUMEYER ET AL. (2004) even use data covering 50 air layers and reaching a height of 60 km.

3.3. Comparison with measured surface pressure

For a comparison of surface pressure variations computed from LM data for the true station height with observed surface pressure it should be considered that the computed curves might contain modelling errors.

In Fig. 4 the difference between modeled and observed surface pressure is shown for the radiosonde stations Meiningen and Munich. More or less regular deviations are visible. On the average the deviations are in the range of ±1 hPa. Larger differences in the order of 2-4 hPa and continuing over several time steps occur from time to time, but never at the same time at both stations.

3.4. Estimate of observation errors using modeled surface pressure curves

Differences between modeled and observed surface pressure curves could originate from modeling errors (see above), but can also be used to identify errors, drifts or additional influences in the barometer record. The pressure recordings at the gravimeter station Medicina are verified using data from the meteorological service which operates a meteorological station at the nearby radiosonde station. This way linear drifts of the pressure sensors at the gravimeter site could be determined (WOLF, pers. comm., 2003).

In Fig. 5 the differences between modelled and observed surface pressure variations are shown for the gravimeter stations Wettzell and Moxa. A deviation between observed and modelled values is clearly visible for Moxa observatory for one of the pressure records. The

Fig. 4. Modelling errors of LM data-derived surface pressure variations, station Munich and Meiningen, year 2003. Deviations of more than 1 hPa do not occur at the same time at the two stations.
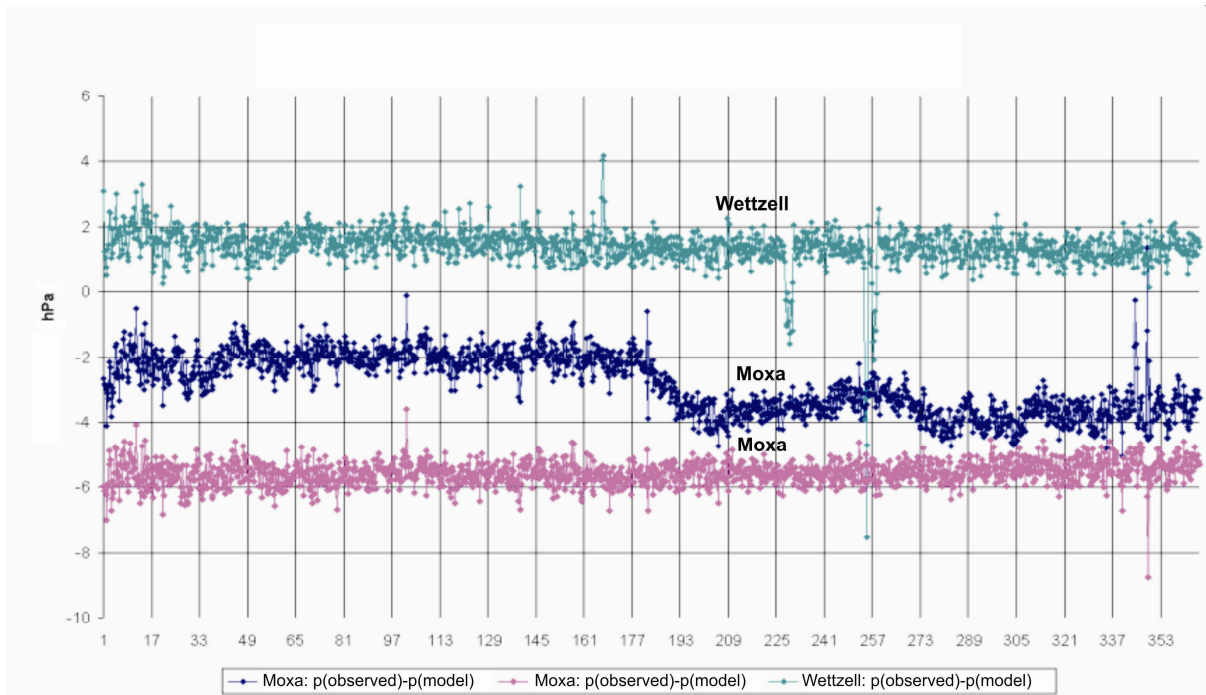
Fig. 5. Difference between modeled and observed surface pressure variations for stations Wettzell and Moxa, year 2003. For one of the records of Moxa observatory a clear deviation of the observed pressure changes from modelled ones can be seen.

second record shows no such discrepancy. On the other hand modelling errors can introduce artificial noise in the gravity residuals when using model data for air mass correction. When the $A_c(t)$-component is computed from (observed) radiosonde data, the resulting curves are smoother.

3.5. Modelling errors due to generalized topography

Another source for deviations between curves derived from LM and radiosonde data might be the generalized topography of the LM due to the model discretization. In present computations the lower boundary of the lowest air layer was on the average 12 m below true station height. This results in an additional air layer in the immediate vicinity of the gravimeter which is not present in reality. In the modelling with radiosonde data not only observed data enter, but the true station height is used.

4. Further factors of influence and consequences

Influence of the area size: As MERRIAM (1992) has pointed out firstly, about 90% of the total air pressure effect in gravity are due to pressure changes in a local zone with a radius of 0.5°. In the model computations discussed here a larger area is taken into account. The radius of 113 km used in this work corresponds to a cap with an angle of 1°.

Influence of earth's curvature: The air mass attraction was computed by SIMON (2003) for a ring model taking into account the curvature of the earth's surface. The differences between the attraction effect derived from the ring and the cylindrical model were neglegible.

Influence of the number of air layers used in the model and height of model cylinder: It is probably a reliable conjecture that the increase in the peak-to-peak amplitude of the annual wave from 1.8 µGal to 2.4 µGal is caused by a more appropriate capture of vertical mass shifts in the 35-layer model. In the computation based on the radiosonde data only 16 air layers enter. Apart from this the smaller height of the meteorological model could also be

a reason for the obtained discrepancies. Therefore comparative computations with global meteorological data as deployed by NEUMEYER ET AL. (2004) would be helpful. Here a maximum model height of 60 km with a larger number of air layers would be possible. Another possibility might be that the maximum height of 31 km in the computation with the radiosonde data is not sufficient for an appropriate precise computation of the $A_c(t)$-component.

Influence of the latitude-dependence of g and separation of $A_c(t)$-component: The influence of the latitude-dependence of g on A(t) and its components has been quantified. This dependence will be taken into account in future computations. The computation of $A_c(t)$ according to (4) and (5) needs still to be done. This requires some more extensive programming.

Assessment of the model comparisons: The authors think that the present model comparisons are necessary and have already yielded valuable information. The research is esp. important as long-term gravity changes become more and more of interest and smaller and smaller gravity signals are chased. The studies need to be continued and should include the model computations by Neumeyer and be done in close cooperation with him.

References

BOY, J.P, GEGOUT, P., AND HINDERER, J., 2002. Reduction of surace gravity from global atmospheric pressure loading. Geophys. J. Int., 149, 534-545.

KLÜGEL, Th., 2003. Bestimmung lokaler Einflüsse in den Zeitreihen inertialer Rotatiossensoren. Final report DFG-Forschungsprojekt LOK-ROT, BKG Frankfurt a.M., Fundamentalstation Wettzell, March 2003.

KRONER C., 1997. Reduktion von Luftdruckeffekten in zeitabhängigen Schwerebeobachtungen. Phd thesis, Institute of Geophysics, TU Clausthal.

KRONER, C. & JENTZSCH, G., 1999. Comparison of different barometric pressure reductions for gravity data and resulting consequences. Phys. Earth Planet. Int., 115, 205-218.

MERRIAM, J., 1992. Atmospheric pressure and gravity. Geophys. J. Int., 109, 488-500.

NEUMEYER J., HAGEDOORN J., LEITLOFF J., AND SCHMIDT T., 2004. Gravity reduction with three-dimensional atmospheric pressure data for precise ground gravity measurements. J. Geodynamics. 38, 437-450.

SIMON, D., 2002. Modelling of the field of gravity variations induced by the seasonal air mass warming during 1998- 2000. Bull. d'Inf. Marées Terr., 136, 10821-10836.

SIMON, D., 2003. Modelling of the gravimetric effects induced by vertical air shifts. Mitt. des BKG Frankfurt a. M., vol. 21.

SIMON, D., 2006. Gravimetric effects induced by vertical air mass shifts at Medicina (1998-2005), Wettzell, Bad Homburg, Moxa, Pecny and Wien (1998-2004), Bull. d'Inf. Marées Terr., this issue.

SMITHONIAN METEOROLOGICAL TABLES, 1951. 6 [th] Revised Edition. Published by the Smithonian Institution, Washington.

SUN, H.-P., 1995. Static deformation and gravity changes at the earth's surface due to atmospheric pressure. Phd thesis Cath. Uni. Louvain, Belgium.

SUN, H.-P., DUCARME, B., AND DEHANT, V., 1995: Correction of the atmospheric pressure on gravity measurements recorded by a superconducting gravimeter at Brussels. Proc. 12th Int. Symp. Earth Tides, Beijing, August 1993, Science Press, Beijing, 317-330